

Development 138, 4167–4178 (2011) doi:10.1242/dev.070391  
 © 2011. Published by The Company of Biologists Ltd

# Gcm/Glide-dependent conversion into glia depends on neural stem cell age, but not on division, triggering a chromatin signature that is conserved in vertebrate glia

Hakima Flici\*, Berra Erkosar\*, Orban Komonyi, Omer Faruk Karatas, Pietro Laneve and Angela Giangrande†

## SUMMARY

Neurons and glia differentiate from multipotent precursors called neural stem cells (NSCs), upon the activation of specific transcription factors. In vitro, it has been shown that NSCs display very plastic features; however, one of the major challenges is to understand the bases of lineage restriction and NSC plasticity in vivo, at the cellular level. We show here that overexpression of the Gcm transcription factor, which controls the glial versus neuronal fate choice, fully and efficiently converts *Drosophila* NSCs towards the glial fate via an intermediate state. Gcm acts in a dose-dependent and autonomous manner by concomitantly repressing the endogenous program and inducing the glial program in the NSC. Most NSCs divide several times to build the embryonic nervous system and eventually enter quiescence: strikingly, the gliogenic potential of Gcm decreases with time and quiescent NSCs are resistant to fate conversion. Together with the fact that Gcm is able to convert mutant NSCs that cannot divide, this indicates that plasticity depends on temporal cues rather than on the mitotic potential. Finally, NSC plasticity involves specific chromatin modifications. The endogenous glial cells, as well as those induced by Gcm overexpression display low levels of histone 3 lysine 9 acetylation (H3K9ac) and *Drosophila* CREB-binding protein (dCBP) Histone Acetyl-Transferase (HAT). Moreover, we show that dCBP targets the H3K9 residue and that high levels of dCBP HAT disrupt gliogenesis. Thus, glial differentiation needs low levels of histone acetylation, a feature shared by vertebrate glia, calling for an epigenetic pathway conserved in evolution.

**KEY WORDS:** Neural stem cells, Glia, *Drosophila*, dCBP, Gcm/Glide, Histone acetylation

## INTRODUCTION

Glia and neurons, the major cell types of the nervous system, share a common precursor population, the NSCs (Bossing et al., 1996; Delaunay et al., 2008; Doe et al., 1998; Rivers et al., 2008; Schmidt et al., 1997). The multipotency of NSCs and their ability to be redirected towards different fates make these cells a promising tool in regenerative medicine; however, the plastic features of this initially homogeneous population needs to be fully understood. In addition, NSC behavior may rely on the experimental asset: while in vitro NSCs self-renew and may produce multiple fates indefinitely, in vivo, they give rise to specific progenies at distinct developmental stages (Gaspard and Vanderhaeghen, 2011). It therefore becomes important to characterize NSC plasticity at cellular and molecular level in vivo. In particular, can NSCs be completely and stably redirected and, if so, is this a constitutive feature? In addition, as histone modifications characterize and control specific transcriptional and differentiative states (Gibney and Nolan, 2010), what is the impact of fate conversion onto the cellular chromatin state?

Transcription factors play an important role in cell fate induction and, more generally, in plasticity (Graf and Enver, 2009); however, the glial versus neuronal decision in the vertebrate central nervous system (CNS) (Rowitch and Kriegstein, 2010) involves a rather

complex gene network, which makes it difficult to assess the role and mode of action of such determinants in vivo (Allen, 2008). The simple *Drosophila* CNS makes it possible to tackle this issue in identified lineages. Moreover, a single transcription factor drives glial differentiation in *Drosophila* embryos: Glial cells missing (Gcm) [also called Glial cell deficient (Glide); referred to as Gcm hereafter] (for a review, see Soustelle and Giangrande, 2007). Gcm is transiently expressed in the lineages that produce glia and acts in the choice between glial and neuronal fates: its loss induces almost complete lack of glia, whereas its overexpression efficiently induces ectopic expression of the *reverse polarity (repo)* pan-glial gene (Bernardoni et al., 1998; Hosoya et al., 1995; Jones et al., 1995; Vincent et al., 1996) and other glial transcripts (Altenhein et al., 2006; Egger et al., 2002; Freeman et al., 2003). The potent gliogenic activity of Gcm therefore provides an ideal asset with which to study lineage restriction and NSC plasticity in vivo.

We here show that *Drosophila* NSCs are stably and completely converted towards the glial fate upon overexpressing Gcm threshold levels. NSCs progressively lose plasticity and can no longer be converted at late embryonic stages, as they enter quiescence. Moreover, NSCs can be converted even in the absence of cell division whereas neurons cannot, showing that plasticity relies on temporal cues rather than on the mitotic potential. Finally, the Gcm pathway triggers low levels of H3K9ac and dCBP, a HAT that triggers H3K9 acetylation. This mark is key for glial development as, increasing H3K9ac levels by specifically overexpressing dCBP in glia, downregulates the expression of glial genes. Thus, a widely expressed HAT is crucial for a cell-specific transcriptional program. Finally, low levels of histone acetylation are conserved in vertebrate glia (Hsieh et al., 2004; Shen et al., 2005), indicating that glial cells need this specific chromatin mark.

Institut de Génétique et de Biologie Moléculaire et Cellulaire, IGBMC/CNRS/INSERM/UDS, BP 10142, 67404 ILLKIRCH, CU de Strasbourg, France.

\*These authors contributed equally to this work

†Author for correspondence (angela@igbmc.fr)

Accepted 28 July 2011

## MATERIALS AND METHODS

### Flies

Flies were raised at 25°C unless otherwise specified. *w<sup>1118</sup>* was the wild type. Transgenic lines were: *UAS-gcm* (one dose: *F184*: 1XGcm; two doses: *M244*: 2XGcm) (Bernardoni et al., 1998); *lbe(K)-Gal4,UAS-GFP* (Baumgardt et al., 2009); *mz/Vum-Gal4* (Landgraf et al., 2003); *apterous-Gal4,UAS-mRFP* (Baumgardt et al., 2007); *gcm<sup>34</sup>/CyO,twi-LacZ* (Vincent et al., 1996); *UAS-dCBP* and *UAS-dCBP-FLAD* (Kumar et al., 2004); *repo-Gal4/TM3* (Sepp et al., 2001); *repo<sup>3692</sup>/TM3ubx-lacZ* (Halter et al., 1995); *repo-Gal4* (Lee and Jones, 2005); and *UAS-mCD8GFP, UAS-eGFP, elav-Gal4, voila-Gal4, hs-Gal4, tub-Gal80ts* and *stg<sup>4</sup>/TM3* (Bloomington Drosophila Stock Center).

### Immunohistochemistry and in situ hybridization

Immunolabeling and in situ hybridization on embryos were as described previously (Bernardoni et al., 1998). Primary antibodies were: mouse(m)- $\alpha$ -Repo (1:50), m- $\alpha$ -Engrailed (1:500) and rat(rt)- $\alpha$ -Elav (1:200) from DSHB; chicken- $\alpha$ -GFP (1:1000), rabbit(rb)- $\alpha$ -RFP (1:500), rb- $\alpha$ -Caspase3 (1:500), m- $\alpha$ -H3K9ac (1:500), rb- $\alpha$ -H3K4me3 (1:500) from Abcam; rb- $\alpha$ -GFP (1:500) (Molecular Probes); rb- $\alpha$ -Phospho histone H3 (Ser10) (1:500, Cell Signaling); rb- $\alpha$ - $\beta$ -gal (1:500, Cappel); rb- $\alpha$ -Eagle [1:500 (Dittrich et al., 1997)]; rb- $\alpha$ -SP2637 and guinea-pig(gp)- $\alpha$ -Nazgul [1:500 (von Hilchen et al., 2010)]; rt- $\alpha$ -Repo [1:1000 (Sen et al., 2005)]; rb- $\alpha$ -Miranda [1:500 (Mollinari et al., 2002)]; gp- $\alpha$ -Deadpan [1:1000, J. Skeath, University of Washington, St Louis, MO]; gp- $\alpha$ -dCBP [1:1000 (Lilja et al., 2003)]; rb- $\alpha$ -dTAF-4 [1:100 (Kokubo et al., 1994)]; m- $\alpha$ -Pol II [1:100 (Puvion-Dutilleul et al., 1997)]; rb- $\alpha$ -dGCN5 [1:500 (Lebedeva et al., 2005)]. Secondary antibodies were FITC-, Cy3-, Cy5-conjugated (1:400, Jackson). For in situ hybridization probes were DIG-*pan* [1:100 (Altenhein et al., 2006)] and DIG-*gcm* [1:100 (Bernardoni et al., 1997)]. Larval CNS proteins were immunolabeled as described previously (Ceron et al., 2001).

### Imaging and cell counting

Images were taken with SP2 and SP5 Leica confocal microscopes. Image processing used Adobe Photoshop CS3. Cells were counted manually using ImageJ. For cell counting, means and standard errors were calculated and analyzed using Student's *t*-test.

### Quantifications

For H3K9ac, H3K4me3 and dCBP relative levels, neurons and glia from the same embryonic VC were subjected to quantification using ImageJ. In brief, masks were generated as a region of interest for each nucleus along the *z*-stack, area ( $\mu\text{m}^2$ ) and fluorescence intensities (pixel number) were measured and summed for all sections. The density of each nucleus was calculated by dividing the mean intensities over the nucleus volume (pixels/ $\mu\text{m}^3$ ). For each embryo, values for all cell types were assigned by taking the highest value as reference and distributed in ten intervals from 1 to 10. The percentage of cells distributed in the different intervals was determined for each cell type for each embryo. This approach provided the best internal control. For quantifications, means and standard errors were calculated and samples were subjected to two-sample Kolmogorov-Smirnov test, which is sensitive to differences between cumulative distribution functions of two compared samples.

### Northern and western blot analysis

*elav-Gal4,UAS-mCD8GFP* and *repo-Gal4,UAS-mCD8GFP* 17 stage embryos were used to purify neuronal and glial cell populations, respectively. Embryos were collected in Schneider's medium +3 mM EDTA and dissociated (Wheaton Dounce homogenizer). Single cell suspensions were obtained upon filtering through 70  $\mu\text{m}$  and 40  $\mu\text{m}$  nets (BD Biosciences) and centrifugation (100 *g*, 5 minutes, 4°C). Cells were washed and collected in Schneider's medium (Gibco BRL), supplemented with 10% FCS (SDMS). GFP+ cells (neurons or glia) were separated with FACSDiVa flow cytometer (Becton Dickinson) (see Fig. S4A in the supplementary material).

For northern blot analyses, RNA was prepared from equal number of neurons and glia using TRIzol Reagent (Invitrogen) following manufacturer's instructions. mRNA levels were determined by northern blot with oligodT probe and using 5S-rRNA as internal control.

For western blot analyses, histone extracts from sorted neurons and glia were obtained as described in Abcam histone extraction protocol. Histone extracts (20  $\mu\text{g}$ ) were separated by 15% SDS-PAGE, transferred onto nitrocellulose membrane and probed with the primary antibodies diluted in 1 $\times$  PBS, 5% bovine serum albumin: m- $\alpha$ -H3K9ac (1:2000), rb- $\alpha$ -H3K4me3 (1:10,000) from Abcam. m- $\alpha$ -H2B (1:10,000, IGBMC) was used for normalization. Signal was detected with Pierce ECL western blotting substrate (Thermo Fisher Scientific, Waltham, MA) using appropriate HRP-conjugated secondary antibodies (1:10,000, Jackson).

### Reverse transcription and qRT-PCR

Total RNA was purified from *repo-Gal4,UAS-mCD8GFP* and *repo-Gal4,UAS-mCD8GFP,UAS-dCBP* embryos by TriReagent (MRC), reverse transcribed by SuperScriptII reverse transcriptase (Invitrogen) using a mix of random hexamers (6  $\mu\text{M}$ ) and oligodT primers (5  $\mu\text{M}$ ), and analyzed by quantitative PCR (qPCR) machine Roche LightCycler480 with Syber Green (Roche) Master mix. For each gene, expression levels were automatically calculated (LightCycler480 Software, release 1.5.0) by calibration to gene-specific standard curves generated on input cDNAs. Collected values, normalized to Actin5C amount, derive from three amplification reactions, each performed on three independent experiments. Primers are described in Table S1 in the supplementary material.

## RESULTS

### Gcm completely converts fly NSCs towards the glial fate

Previous studies showed that Gcm overexpression in the neuroepithelium prior to NSC birth induces the expression of glial markers through unknown mechanisms (Hosoya et al., 1995; Miller et al., 1998) (see the territory of expression as revealed by GFP labeling in Fig. S1A in the supplementary material). To understand the bases of lineage restriction and NSC plasticity, we specifically overexpressed Gcm with Gal4 drivers active in most (*voila-Gal4*) (Grosjean et al., 2001) (Fig. 1D, see Fig. S1D in the supplementary material) or in subsets of NSCs (*embryonic lethal abnormal vision-Gal4* or *elav-Gal4*) (Berger et al., 2007) (see Fig. S1B,C in the supplementary material). The Repo pan-glial marker is massively induced at ectopic positions, at the expense of the neuronal markers (see Fig. S2E,F in the supplementary material; data not shown), a phenotype that is stronger with the pan-neuroblast *voila-Gal4* driver than with *elav-Gal4* (Campbell et al., 1994) (Fig. 1A-C). Most *Drosophila* CNS glia arise from neuroglioblasts (NGBs) and few from glioblasts (GBs); however, the vast majority of embryonic NSCs only produces neurons [neuroblasts (NBs)] (Bossing et al., 1996; Schmidt et al., 1997). This strongly suggests that the massive number of ectopic glia also arise from precursors that only produce neurons. To verify this hypothesis, we overexpressed Gcm and used two lineage-specific markers, Eagle (Eg) and Engrailed (En), to identify unequivocally pure NBs (Doe, 1992). The so-called Thoracic 2-4 and 3-3 lineages, which are Eg(+),En(-) (Higashijima et al., 1996), clearly show Repo labeling, demonstrating that NBs overexpressing Gcm can produce glia at the expense of neurons (Fig. 1J-O).

We then asked how does Gcm induce glia and found that NSCs overexpressing Gcm lose their stemness, revealed by downregulation of the mitotic marker (PH3) (Fig. 1E) and of the NB markers Miranda (Mira) (Shen et al., 1997) (Fig. 1H,I) and Deadpan (Dpn) (Bier et al., 1992) (data not shown). As overexpression of Gcm begins, few cells express the glial marker ectopically and NBs are still present; however, most of them express both NB and glial markers. Later on, many more cells express the glial marker ectopically and only few cells express the NB marker, most of them also expressing the glial marker (Fig. 1F-I). The progressive increase of ectopic glial cells at the expense of NBs strongly suggests that the NBs initially express their program,

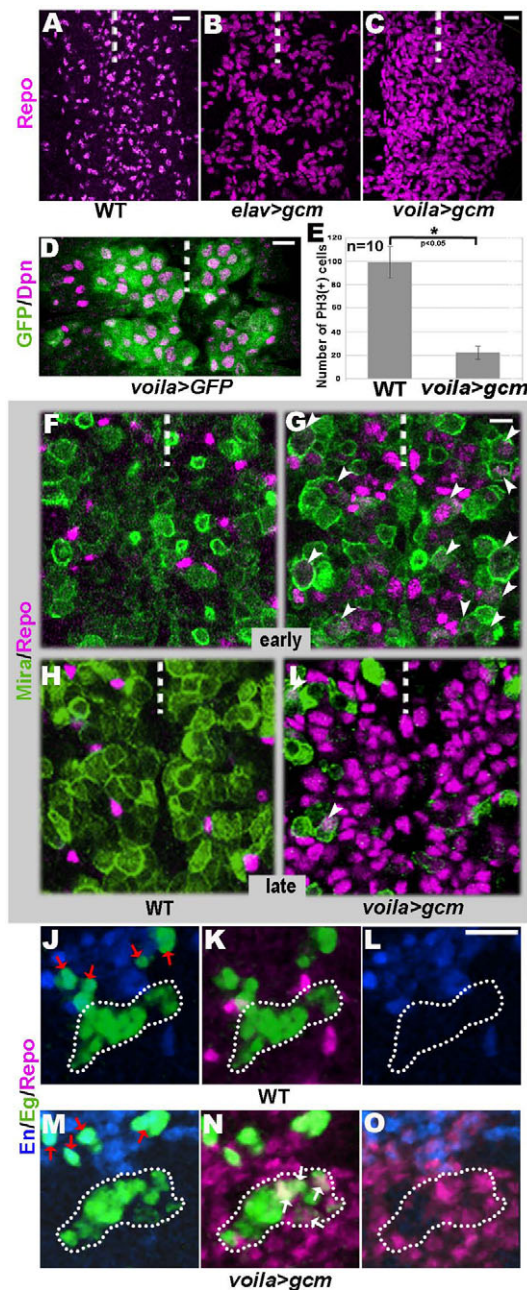


**Fig. 1. Gcm redirects NSCs towards the glial fate.** (A–C) Stage 16 embryos labeled with Repo (magenta) in: (A) control (wild type), (B) *elav-Gal4>UAS-gcm* (*elav>gcm*) and (C) *voila-Gal4>UAS-gcm* (*voila>gcm*) embryos. (D) *voila-Gal4>UAS-GFP* (*voila>GFP*) stage 13 embryo labeled with GFP (green) and NB marker Deadpan (Dpn, magenta). (E) The number of dividing, phospho-histone H3 (Ser10)-positive cells [PH3(+)], in the ventral cord (VC) of wild-type and *voila>gcm* stage 15 embryos. Data are mean  $\pm$  s.e.m. (F–I) Control (wild type) and *voila-Gal4>UAS-gcm* (*voila>gcm*) embryos labeled with the Miranda (Mira, green) NB marker and Repo (magenta) at early (F,G) and late (H,I) stages. Note the presence of Mira(+),Repo(+) cells (arrowheads) in *voila>gcm* (G,I) but not in the control embryo (F,H). (J–O) Control (wild type) (J–L) and *voila>gcm* (M–O) stage 14 embryos labeled with lineage-specific markers Eagle (Eg, green) and Engrailed (En, blue). Repo is in magenta. Broken lines indicate the progenies of pure NBs [Eg(+),En(-)], whereas red arrows indicate the progenies of Eg(+),En(+) lineages, one of which is an NGB. White arrows indicate ectopic gliogenesis in pure NBs (N). All panels show confocal projections, anterior is towards the top, broken line indicates midline. Unless specified, all figures show ventral views; error bars indicate  $\pm$  s.e.m., asterisk indicates statistical significance. Scale bars: 10  $\mu$ m.

then co-express the glial and the NB ones and finally only express the glial program. NSC conversion is dose-dependent and cell autonomous: it increases when two *UAS-gcm* reporters are used (see Fig. S2A,B in the supplementary material) and is confined to the cells overexpressing Gcm (see Fig. S2I,J in the supplementary material). Finally, the induction of late glial genes [Nazgul, SP2637 (von Hilchen et al., 2010), *pain* (Altenhein et al., 2006), Draper,  $\beta$ -Moody (Freeman et al., 2003)] (see Fig. S2C,D,G,H,K,L in the supplementary material and data not shown) confirms that stable and complete transformation has occurred. Thus, NSCs are fully converted into glia by the Gcm transcription factor.

### Gcm cannot convert neurons into glia

Recent data indicate that somatic cells as fibroblast can transdifferentiate into neurons (Vierbuchen et al., 2010) and that one subtype of neurons can transdifferentiate into another (Wright

et al., 2010). As the used neuroblast drivers continue to be expressed at late embryonic stages in post-mitotic cells (see Fig. S1E–G in the supplementary material) (Berger et al., 2007), we asked whether the observed phenotype may also arise from neurons, due to transdifferentiation and/or to reversion towards a more immature state.

To address this issue directly, we used Gal4 drivers that are expressed in post-mitotic cells but not in their precursors: *apterous-Gal4* (*ap-Gal4*) and *mzVUM-Gal4* are specific to two motoneuron subsets (Baumgardt et al., 2007; Landgraf et al., 2003). These drivers are clearly able to induce Gcm overexpression upon crossing with *UAS-gcm* flies (Fig. 2E–H); however, they never induce ectopic Repo labeling (Fig. 2A–D), regardless of Gcm dose (Fig. 2E–H). Because these drivers are expressed at relatively late embryonic stages, we wondered whether the glial Repo marker might be induced in the larva. Even at that stage, however, no fate conversion was observed (Fig. 2L,J). Interestingly, neurons overexpressing Gcm enter the apoptotic pathway via Caspase 3 activation (Cohen, 1997) (Fig. 2K,L). In summary, neurons cannot be reprogrammed by Gcm.

### NSC plasticity decreases during development

We then asked whether NSCs remain plastic throughout their life. The *lbe(K)-Gal4* line (Baumgardt et al., 2009) is expressed in an identified lineage, the so-called 5–6. In the thorax, the (5–6T) NSC is born by stage 9 and divides until stage 15. The TARGET system, based on a ubiquitously expressed thermosensitive Gal80 allele (*tub-Gal80ts*), makes it possible to repress the Gal4 activity at specific stages (McGuire et al., 2003). *Gal80ts,lbe(K)-Gal4>UAS-gcm* synchronized embryos were raised at the permissive temperature (18°C), shifted to the restrictive temperature (29°C) to induce Gcm expression at different stages (2 hours, 4 hours, 6 hours after egg collection) and let differentiate at that temperature (Fig. 3A–D). Under each condition, we waited for at least 9 hours, in order to allow sufficient time for Gcm activation [Gal80-induced repression is known to rapidly fade away after the shift (McGuire et al., 2003)]. Control animals not expressing Gcm were submitted

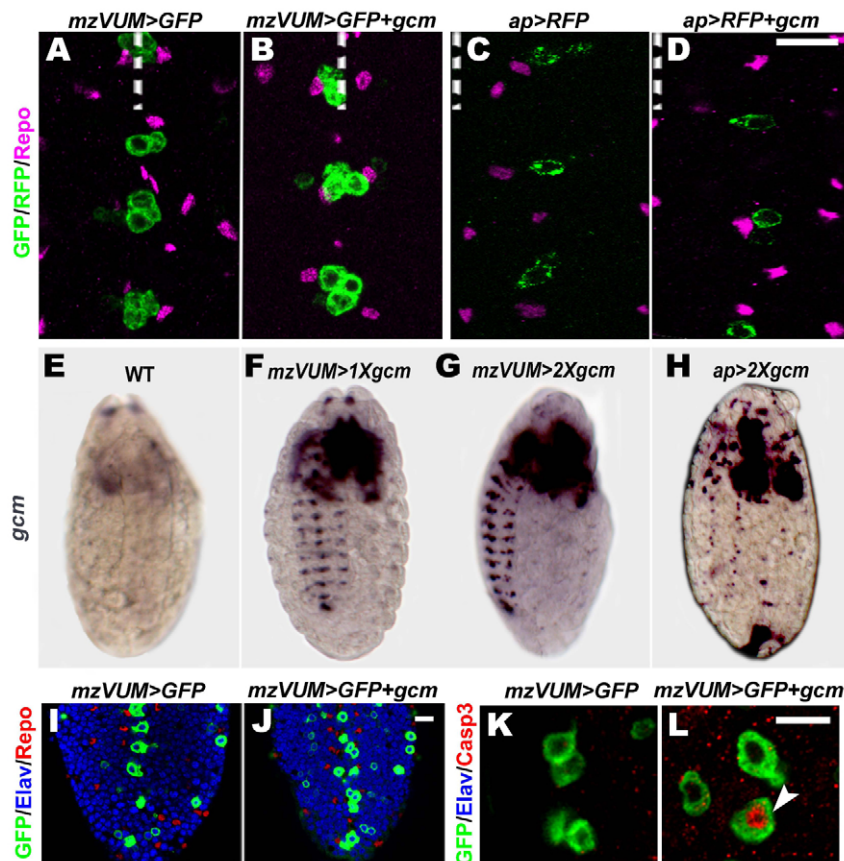


**Fig. 2. Gcm cannot reprogram post-mitotic neurons.** (A–D) Confocal sections of stage 16 embryos. No ectopic Repo (magenta) is observed upon Gcm overexpression using two different post-mitotic drivers, *mzVUM* and *apterous* (*ap*); neurons are visualized with GFP/RFP (green). Compare *mzVUM-Gal4>UAS-GFP* (*mzVUM>GFP*) control embryo (B) with *mzVUM-Gal4>UAS-GFP;UAS-gcm* (*mzVUM>GFP+gcm*) embryo (A) and *ap-Gal4>UAS-RFP* (*ap>RFP*) control embryo (D) with *ap-Gal4>UAS-RFP;UAS-gcm* (*ap>RFP+gcm*) embryo (C). (E–H) *gcm* RNA expression pattern in control embryo (wild type) (E) compared with Gcm-overexpressing embryos under *mzVUM-Gal4* and *ap-Gal4* drivers (F–H). *gcm* RNA levels increase when two *UAS-gcm* reporters are used [compare (*mzVUM>1Xgcm*) (F) to (*mzVUM>2Xgcm*) (G)]. (I, J) Confocal sections of 3rd instar larvae show no ectopic Repo (red) upon Gcm overexpression in post-mitotic neurons; neurons are visualized with Elav (blue), compare *mzVUM>GFP* (I) with *mzVUM>GFP+gcm* (J). (K, L) *mzVUM* neurons die by apoptosis upon Gcm overexpression, see the GFP(+), activated Caspase3 (Casp3, red)(+) cells (arrowhead) in L, but not in control animals (K). Scale bars: 10 μm.

to the same regimens for comparison. These results were also compared with those obtained upon constitutive Gcm expression in that lineage (Fig. 3B–D). Clearly, glial induction is most successful when the NSC is challenged with Gcm throughout development. Among the different shifts, the earliest one (2 hours) is more successful than a late one (4 hours) and in the latest shift (6 hours), no ectopic glia can be induced. Thus, the 5–6T NSC becomes less plastic with time.

This particular NSC is eliminated through programmed cell death at stage 15 (Karlsson et al., 2010), whereas others enter the quiescent state and resume proliferation during the larval stages, to build the adult nervous system (Sousa-Nunes et al., 2011). This cellular state is conserved throughout evolution, as quiescent NSCs are typical of the adult mammalian brain (Morshead et al., 1994). We asked whether plasticity decreases with time in all NSCs and induced pulses of Gcm expression at different stages using the heat shock (hs) promoter. We submitted *hs-Gal4>UAS-gcm* synchronized embryos to a 1-hour heat shock at the time NBs first arise and found that most if not all embryonic territories massively produce ectopic glia (see Fig. S3C in the supplementary material). Starting from a 6–7 hours after egg laying (AEL) heat shock, the strong gliogenic potential of Gcm is limited to the neurogenic region (Fig. 3E,F), where a single pulse of Gcm expression is sufficient to induce a stable and complete glial fate (see Fig. S3A,B in the supplementary material). Upon a shock at 8–9 hours AEL, the number of ectopic glia decreases considerably (Fig. 3G), even though in wild-type animals NSCs are still present and actively proliferating at this stage (Fig. 3I,J). Finally, upon a later shock (10–11 hours AEL, which corresponds to embryonic stage 14), almost no cells express ectopic Repo (Fig. 3H), even though Gcm

expression is induced (see Fig. S3D in the supplementary material). The rare ectopic Repo(+) cells are also labeled by the Dpn and Mira NB markers, therefore expressing an intermediate fate (Fig. 3K). By these late stages, the number of NBs is still high but that of dividing NBs rapidly decreases (Fig. 3I,J) and that of quiescent NBs, recognized by Mira, Dpn labeling and by morphology [elongated shape and long cytoplasmic extension (Tsuiji et al., 2008)], increases significantly (Fig. 3M–Q). Notably, none of the Repo(+), Dpn(+) cells is a quiescent cell (Fig. 3L). Thus, late NSCs can be poorly redirected towards the glial fate. Altogether, these data show that NSC plasticity becomes restricted with time.

### NSC plasticity does not require cell division

During development, most novel fates are implemented upon cell division. We therefore asked whether NSC plasticity depends on cell cycle using a mutation in which NBs are generated but cannot divide. Previous studies have shown that NBs mutant for the String (Stg) protein, a Cdc25 phosphatase that activates a cyclin-dependent kinase and therefore mitosis (Edgar and O'Farrell, 1990), are blocked before their first division (Akiyama-Oda et al., 2000; Berger et al., 2010). Strikingly, Gcm overexpression does induce ectopic Repo labeling in *stg* mutant NBs (Fig. 4A–D,H).

We then asked whether the presumptive non-dividing NBs can be fully converted and found that the late glial marker SP2637 is also induced (Fig. 4E). Moreover, similar to wild-type NSCs challenged with Gcm, the NB fate is downregulated in *stg* embryos overexpressing Gcm (Fig. 4F,G). Interestingly, even at these late stages, some non-dividing NBs simultaneously express a glial and a NB marker, a phenotype that is rarely observed in *stg* animals (Fig. 4F,G, arrowheads). Moreover, 14% of the cells that express

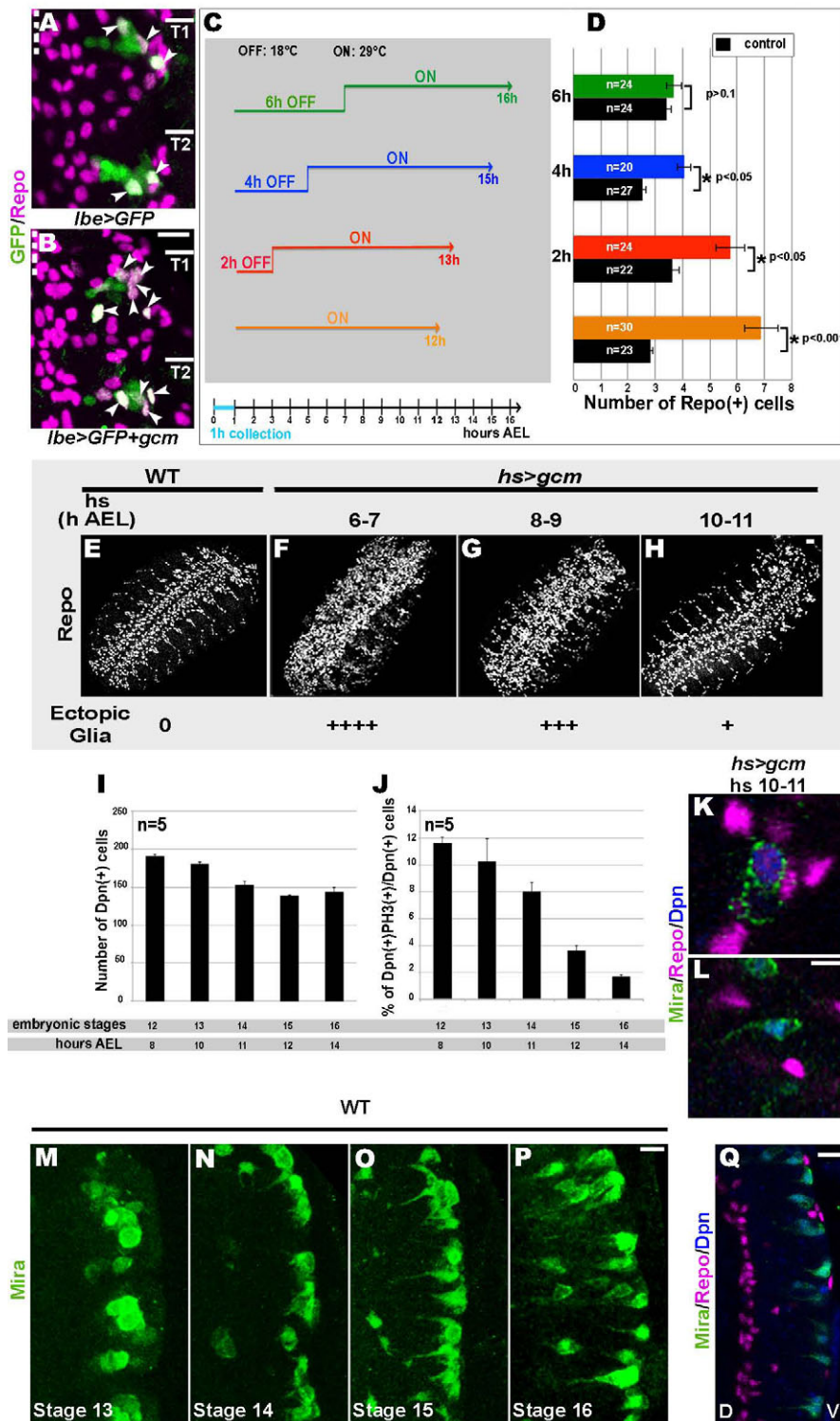


**Fig. 3. NSC plasticity decreases during development.** (A,B) Projections of stage 16 embryos show Repo (magenta) expression upon Gcm overexpression in the 5-6T lineage (arrowheads) using the *lbe(K)-Gal4* driver. Compare *lbe(K)-Gal4>UAS-GFP* (*lbe>GFP*) control embryo (A) with *lbe(K)-Gal4>UAS-GFP;UAS-gcm* (*lbe>GFP+gcm*) (B). The 5-6T lineage was visualized by GFP (green). (C,D) Induction of ectopic Repo upon Gcm overexpression in the 5-6T lineage at different embryonic stages using the TARGET system, compare *Gal80ts,lbe(K)-Gal4>UAS-GFP* (*Gal80ts,lbe>GFP*) control with *Gal80ts,lbe(K)-Gal4>UAS-GFP;UAS-gcm* (*Gal80ts,lbe>GFP+gcm*) animals treated in the same way. Embryos were collected for 1 hour and raised at 18°C (OFF: repressive temperature) then shifted to 29°C (ON: permissive temperature) to induce Gcm expression at different stages, as indicated, until stage 16. Color coding indicates the different times at which the temperature was shifted: 2 hours (red), 4 hours (blue) and 6 hours (green) after egg collection. 0 h indicates embryos kept at 29°C from birth (orange). (D) The number of Repo(+) cells generated from the 5-6T lineage in control (black columns) and Gcm-overexpressing (colored columns) embryos. The number of Repo(+) cells is similar in overexpressing and control embryos upon a temperature shift at 6 hours AEL (green). n indicates the number of 5-6T lineages. (E-H) Projections showing Repo (white) in control, *hs-Gal4>W<sup>1118</sup>* (WT) (E) and *hs-Gal4>UAS-gcm* (*hs>gcm*) embryos (F-H) upon 1 hour heat shock (hs) at the indicated times (hours AEL) then fixed 5 hours after the heat pulse. (I,J) The graphs show the number of NBs [Dpn(+)] (I) and the percentage of mitotic NBs [PH3(+),Dpn(+)] (J) in the thorax of different embryonic stages. n indicates the number of embryos. Data are mean±s.e.m. (K,L) *hs>gcm* embryo fixed 5 hours after the hs, showing colocalization between Repo (magenta) and Dpn (blue) in round Mira(+) cells but not in elongated Mira(+) NBs. (M-Q) Projections showing thoracic NBs labeled by Mira (green) at the indicated embryonic stages; lateral views, dorsal (D) towards the left, ventral (V). Note the progressive accumulation of quiescent NBs [elongated Mira(+) cells] during development. Scale bars: 10 µm.

Repo also express the neuronal marker Elav, a phenotype that is also very rarely observed in *s/g* or wild-type embryos, as well as in wild-type embryos overexpressing Gcm (Fig. 4I and data not shown). Thus, plasticity is not connected to the mitotic potential.

### Neurons and glia display different H3K9ac levels

Increasing evidence suggests that transcriptional developmental programs are associated with specific chromatin landmarks (for a review, see Lessard and Crabtree, 2010) and it has been shown that

low levels of histone acetylation characterize vertebrate glial cells (Hsieh et al., 2004; Jakob, 2011). We therefore determined the overall histone acetylation profiles of wild-type neurons and glia. The CNS displays high levels of H3K9ac (Qi et al., 2004), which is abundant in euchromatin. We labeled fully differentiated neurons and glia with an anti-H3K9ac antibody and found that glia display lower H3K9ac levels compared with neurons (Fig. 5A-C). To gain quantitative information, we identified ten levels of H3K9ac intensity (see Materials and methods for detailed description) upon

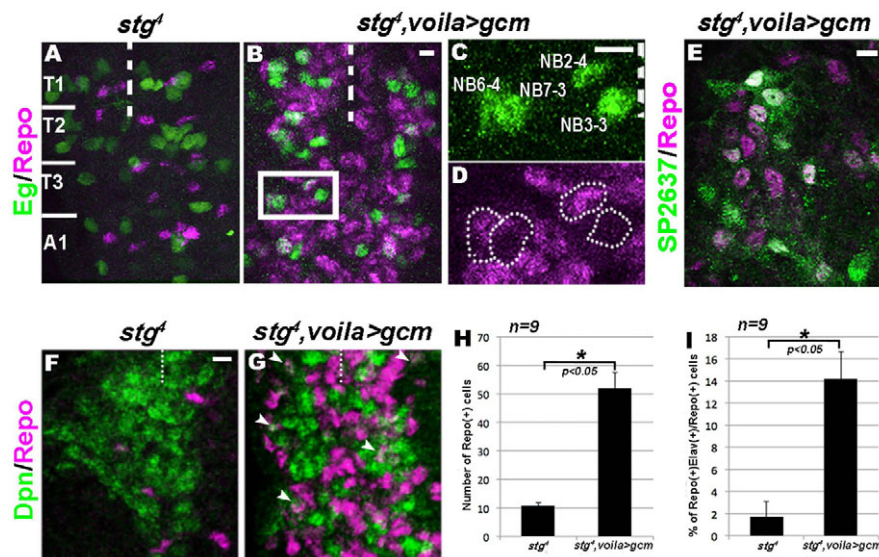


**Fig. 4. NSC conversion does not require cell division.** (A–D) Projections show *stg4* (A) and *stg4,voila>Gal4>UAS-gcm* (*stg4,voila>gcm*) (B) stage 15 embryos labeled with Eg (green) lineage-specific tracer and Repo (magenta). (C,D) The four Eg-specific lineages present in each thoracic hemisegment (boxed in B; note ectopic gliogenesis in undivided NBs (magenta)). (E) Confocal section from *stg4,voila>gcm* VC shows glial subsets expressing late glial marker SP2637 (green). (F,G) Confocal sections showing thoracic segments of stage 15 embryos. Note the colocalization between Repo and Dpn in *stg4,voila>gcm* but not in *stg4* embryos (G). Scale bars: 10  $\mu$ m. (H,I) The graphs show the number of Repo(+) cells (H) and the percentage of Repo(+)Elav(+) cells (I), in the VC of *stg4* and *stg4,voila>gcm* embryos. Data are mean  $\pm$  s.e.m.

comparing glial cells and neurons within the same embryo. Clearly, most glial cells display relatively low levels of H3K9ac compared with neurons (Fig. 5E, embryo  $n=6$ ). Finally, we confirmed this result by western blot on histone extracts from purified neurons and glia (see Fig. S4 in the supplementary material, Fig. 5K). The purity of such populations was validated by using cell-specific markers (see Fig. S4B,C in the supplementary material).

Interestingly, the levels of H3K4me3, which specifically marks transcriptionally active genes (Lessard and Crabtree, 2010), are similar in neurons and glia (embryo  $n=5$ ,  $P>0.08$ , Fig. 5I), as confirmed by western blot (Fig. 5L). Moreover, H3K9ac partially colocalizes within the cell with H3K4me3 [32.8% colocalization in neurons and 34.4% in glia,  $n=10$  (see Fig. S5A–C, Movies 1 and 2 in the supplementary material)], which we confirmed in 3D reconstructions of glial and neuronal nuclei (see Fig. S5A,B in the supplementary material). These data imply that different acetylation levels do not reflect global differences in transcription activity between neurons and glia, and, to further validate this, we showed that the total mRNA levels are not higher in neurons than in glia (Fig. 5J). Finally, we quantified H3K9me3 levels, as a mark of repression and heterochromatin (Lessard and Crabtree, 2010), and found no significant difference between neurons and glia either (embryo  $n=4$ , see Fig. S5D in the supplementary material). In summary, neurons and glia have distinct properties in terms of chromatin marks, which are independent from the overall transcriptional state.

### The Gcm pathway controls the levels of H3K9ac

We then asked whether fate conversion upon Gcm overexpression results in changes in histone acetylation, i.e. whether ectopic glia show low H3K9ac levels. As we wanted to compare the acetylation state of endogenous and ectopic glia within the same animal, we labeled embryos (*elav-Gal4>UAS-GFP;UAS-gcm*) with GFP and Repo [endogenous glia: GFP(–),Repo(+), ectopic glia: GFP(+),Repo(+)] (Fig. 5D) and found that both endogenous and ectopic glia display low H3K9ac levels (embryo  $n=5$ , Fig. 5F).

Several pieces of evidence indicate that low H3K9ac specifically characterizes glial identity. First, the dose of Gcm impacts onto the number of cells showing low H3K9ac levels [compare the H3K9ac levels upon overexpressing two (Fig. 5F) and one (see Fig. S6G in

the supplementary material) dose of Gcm], as it impacts onto the number of ectopic glia. Second, post-mitotic Gcm expression, which does not induce reprogramming, does not change H3K9ac levels (even with two Gcm doses) (see Fig. S6A–C in the supplementary material). Third, if alterations in H3K9ac levels were to reflect fate changes, *gcm* animals, in which presumptive glial cells are converted into neurons, should display opposite changes in the H3K9ac profiles. *gcm<sup>34</sup>* animals maintain *lacZ* expression from a P-element inserted at the *gcm* locus, thereby allowing us to identify the cells that transform into ectopic neurons [*lacZ*(+),Repo(–),Elav(+)] (Vincent et al., 1996). These cells indeed display high H3K9ac levels, similar to the endogenous neurons (embryo  $n=5$ ) or from wild-type animals (Fig. 5G). Finally, we analyzed the H3K9ac levels in animals that lack the Repo protein, which show no glia to neuron conversion, using a null mutant that maintains *lacZ* expression from a P-element at the *repo* locus (Campbell et al., 1994; Halter et al., 1995). In this mutant, the *lacZ*(+) cells still show low levels of H3K9ac compared with neurons and similar to the wild-type glia (embryo  $n=5$ ) (Fig. 5H). In summary, the Gcm pathway induces global changes in H3K9ac levels.

### Neurons and glia display distinct dCBP levels that are controlled by the Gcm pathway

dCBP (Akamaru et al., 1997) constitutes a likely candidate for the above-described histone modification, as its orthologs, CBP/p300 HATs, trigger the acetylation of H3K9 (Wang et al., 2010). We therefore overexpressed dCBP in glia (*repo>dCBP*) and demonstrated for the first time in vivo that it induces high levels of H3K9ac (Fig. 6E,F,H,I,K,L), whereas overexpressing a dCBP mutant form that lacks its HAT activity (dCBP-FLAD) (Kumar et al., 2004) does not (Fig. 6G,J,M). Accordingly, *nej<sup>3</sup>* embryos, which do not express zygotic dCBP, show reduced levels of H3K9ac, which are due to the maternal load (see Fig. S7A–D in the supplementary material). These data suggest that the dCBP HAT contributes to the different H3K9ac levels observed in neurons and glia.

If neurons and glia display distinct properties in terms of histone acetylation, the HAT responsible for such marking must either act in a different way or accumulate at different levels in these cell

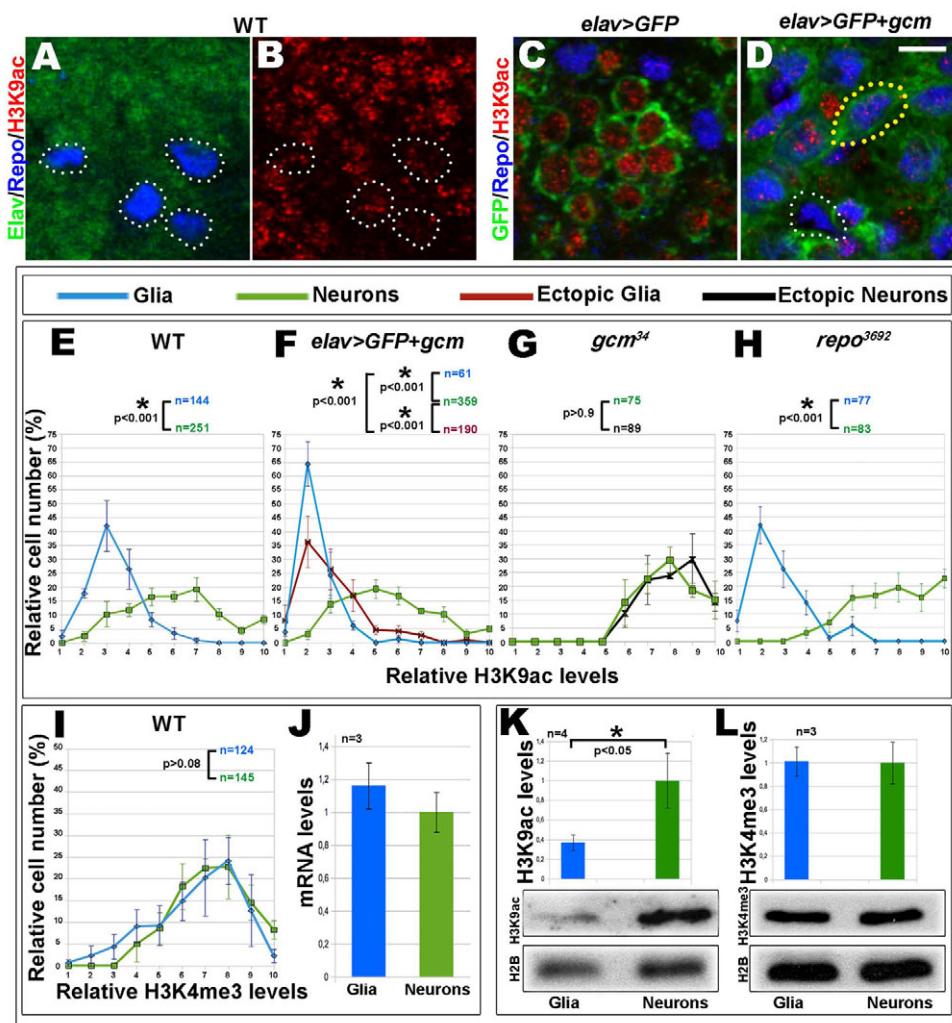


**Fig. 5. Levels of chromatin marks in neurons and glia from wild-type, *gcm*, *repo* and *Gcm*-overexpressing embryos.** (A-D) Confocal sections (stage 17) showing the profile of H3K9ac (red) in glia (Repo, blue) and neurons (green) of control embryos: wild type (A,B) and *elav-Gal4>UAS-mCD8GFP* (*elav>GFP*) (C). (D) *Gcm*-overexpressing embryos: *elav-Gal4>UASmCD8GFP;UAS-gcm* (*elav>GFP+gcm*). Neurons are visualized with Elav in A and GFP in C,D. White and yellow dotted circles indicate endogenous [Repo(+)] and ectopic glia [GFP(+),Repo(+)], respectively. (E-H) H3K9ac levels in neurons (green), glia (blue), ectopic-glia (red) and ectopic-neurons (black) quantified and plotted for wild-type (E), *Gcm*-overexpressing (*elav>GFP+gcm*) (F), *gcm* (*gcm<sup>34</sup>*) (G) and *repo* (*repo<sup>3692</sup>*) (H) embryos; n indicates the number of cells. (I) Quantified neuronal and glial H3K4me3 levels in wild-type embryos. For graphs in E-I, labeling intensity was arbitrarily subdivided into ten levels going from lowest (1) to highest (10) (x-axis), y-axis indicates the percentage of cells for each intensity (see Materials and methods). Data are mean $\pm$ s.e.m. (J) Comparison of neuronal and glial mRNA levels upon northern blot. mRNA levels were normalized to those of neurons arbitrarily chosen as '1'. (K,L) Western blot analysis of H3K9ac and H3K4me3 in histone extracts from FACSed glia and neurons. Neurons display higher levels of H3K9ac than glia (K). Neurons and glia show same levels of H3K4me3 (L). Quantifications of western blot results; mean value is shown in graphs  $\pm$ s.e.m.; n indicates the number of experiments. H2B was used as the loading control. Scale bar: 5  $\mu$ m.

types. Indeed, most neurons display higher dCBP levels than glia (embryo  $n=4$ , Fig. 6A). Moreover, and in line with the above data, ectopic glia induced by *Gcm* overexpression exhibit dCBP levels similar to those of endogenous glia ( $n=5$ , Fig. 6B); upon ectopic neurogenesis induced by *gcm* loss, dCBP levels are similar to those of endogenous neurons (embryo  $n=5$ , Fig. 6C). Finally, dCBP levels do not change in *repo* animals (embryo  $n=5$ ) (Fig. 6D) or upon *Gcm* overexpression in neurons (see Fig. S6D-F in the supplementary material). Thus, like the H3K9ac levels, dCBP levels also change upon the acquisition of specific cell fates. Interestingly, the levels of dGCN5, another major HAT involved in H3K9 acetylation (Carre et al., 2005) are not different between neurons and glia, and dGCN5 overexpression does not affect

H3K9ac levels (see Fig. S8A-C,F,G in the supplementary material). Thus, neurons and glia display distinct levels of dCBP, a HAT that affects H3K9ac levels, and this depends on the *Gcm* pathway.

### High dCBP levels affect glial-specific gene expression

The fact that glia display low dCBP and H3K9ac levels and that fate conversion is accompanied by corresponding changes in those levels suggests that low dCBP levels have a physiological relevance in glial differentiation. We therefore determined the consequences of dCBP overexpression in glia and found that this leads to an obvious increase in H3K9ac levels in glial cells and to embryonic lethality. The few larval escapers do not show the

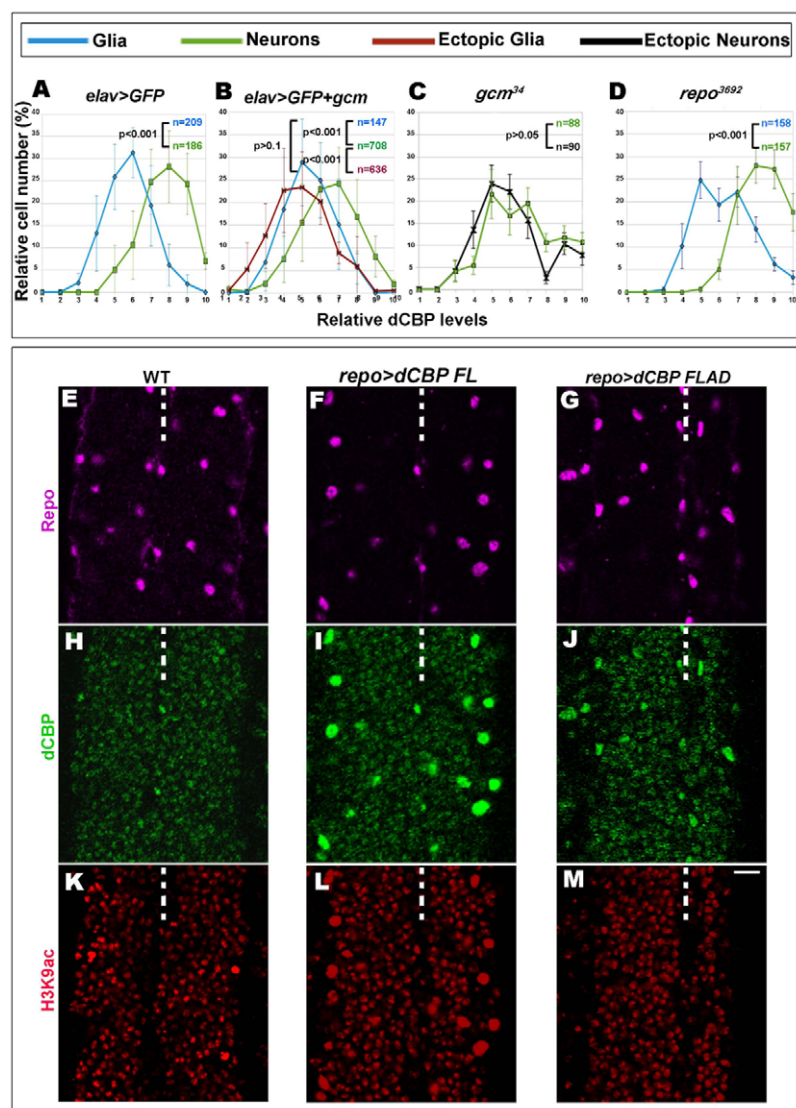


**Fig. 6. dCBP levels in neurons and glia.** (A-D) Graphs show dCBP levels in neurons (green), glia (blue), ectopic glia (red) and ectopic neurons (black) quantified and plotted for control (wild type) (A), Gcm-overexpressing (*elav>GFP+gcm*) (B), *gcm* (*gcm<sup>34</sup>*) (C) and *repo* (*repo<sup>3692</sup>*) embryos (D). Data are mean  $\pm$  s.e.m. (E-M) Confocal sections from control embryos (wild type), embryos overexpressing wild-type (*repo>dCBP*) or inactive dCBP (*repo>dCBP-FLAD*), labeled with Repo (magenta), dCBP (red) and H3K9ac (cyan). Scale bar: 10  $\mu$ m.

typical contractions generated by neuronal activity, showing that glial cells cannot sustain high dCBP levels. Such a phenotype depends on the HAT activity, as animals overexpressing the dCBP-FLAD transgene survive until adulthood. The number of Repo(+) cells does not change, nor is the caspase pathway activated, indicating that high dCBP levels do not merely affect the number of glia by inducing glial cell death (see Fig. S7E-G in the supplementary material).

We then asked whether high dCBP levels impact onto the expression of glial-specific genes. Clearly, the levels of *pain*, which is specific to subperineurial and nerve root glia (Beckervordersandforth et al., 2008), of *Nazgul*, which is specific for longitudinal and cell body glia (von Hilchen et al., 2010), and of *Repo* decrease upon wild-type dCBP, but not upon HAT inactive dCBP overexpression (Fig. 7A-I). The levels of *SP2637*, a nuclear factor that is specific for surface-associated and nerve root glia (von Hilchen et al., 2010) remain unmodified (Fig. 7J,K). Thus, the expression of most but not all tested glial genes is downregulated by high dCBP levels. By contrast, three ubiquitously expressed genes: DNA Pol II (Puvion-Dutilleul et al., 1997), dGCN5 (Xu et al., 1998) and the dTAF-4 subunit of the TFIID complex that initiates transcription (Kokubo et al.,

1994), are not affected (Fig. 7M-R). In order to quantify and extend these findings, we performed quantitative RT-PCR on nine glial-specific transcripts: *repo*,  $\beta$ -*moody*, which is specific to surface glia (Bainton et al., 2005), *draper*, which is specific to lateral glia (Freeman et al., 2003), *pain*, *nazgul*, *SP2637* and three glial transcripts identified by microarrays (Altenhein et al., 2006; Egger et al., 2002; Freeman et al., 2003). As above, dCBP overexpression affects the levels of all transcripts except those of *SP2637* (Fig. 7L). As a negative control, we also analyzed the neuronal *elav* gene, the levels of which are not changed. These data show that high levels of dCBP HAT induce lethality and affect the glial transcriptional program.

## DISCUSSION

Understanding the biology and the potential of stem cells of specific origins is a key issue in basic science and in regenerative medicine. We here show that NSCs can be fully and stably redirected towards the glial fate in vivo, via a transient, intermediate, state, upon the expression of a single transcription factor. NSC plasticity is temporally controlled and quiescent NSCs cannot be converted; however, plasticity is independent of cell division. Finally, the acquisition of the glial fate involves low

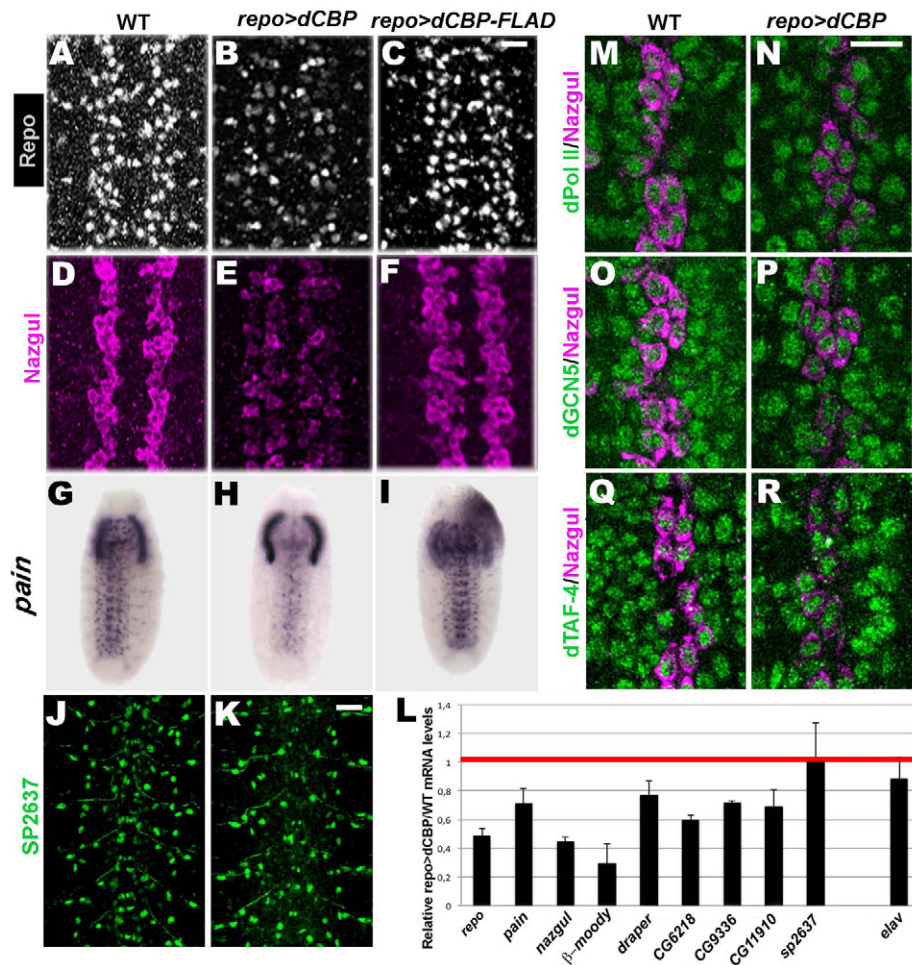


**Fig. 7. dCBP overexpression downregulates the expression of glial-specific genes. (A-I,M-R)** The expression of the glial markers: Repo (white) (A-C), Nazgul (magenta) (D-F,M-R) (same embryos as in A-C) and *pain* (in situ hybridization) (G-I) decrease drastically upon dCBP (B,E,H) but not dCBP-FLAD (C,F,I) overexpression. (J,K) The glial marker SP2637 (green) and the ubiquitously expressed genes dPol II, dGCN5 and dTAF-4 (green) are not affected upon dCBP overexpression. Compare K with J. Scale bars: 20  $\mu$ m. (L) Relative expression of glial markers upon dCBP overexpression in glia. *elav* is used as a control for the expression of a neuronal gene. For wild-type and dCBP-overexpressing embryos, the amount of each transcript was normalized to that of Actin. The wild-type values were arbitrarily taken as 1 (red line) and, for each transcript, the ratio *repo>dCBP/WT* was determined in three independent experiments (columns show average values  $\pm$  s.e.m.).

histone acetylation, a chromatin modification that is conserved throughout evolution, emphasizing the importance of this mark in glial cells.

### NSCs can be fully redirected towards the glial fate in vivo

NSCs produce the different types of neurons and glia that form the nervous system. These precursors can be converted into induced pluripotent cells (Kim et al., 2009) and even into monocytes, a differentiated fate of an unrelated somatic lineage (Forsberg et al., 2010); however, the in vitro behavior may differ markedly from the in vivo situation. For example, the Achaete-Scute Complex homolog-like 1 transcription factor promotes the expression of oligodendrocyte features upon retroviral injection in the dentate gyrus, but promotes neuronal differentiation from the same progenitors in vitro (Jessberger et al., 2008). The use of NB-specific drivers, markers and conditional overexpression protocols, allows us to demonstrate that a single transcription factor can fully convert NSCs into glia in a dose-dependent manner. High Gcm levels probably enable this transcription factor to counteract the endogenous transcriptional program and/or to compensate for the absence of cell-specific co-factors. Quantitative regulation is also required in physiological conditions; for example, the nuclear protein Hucklebein enhances the gliogenic potential of Gcm upon triggering its positive autoregulation in a specific lineage (De Iaco et al., 2006). The present study therefore shows for the first time that NSCs can be

completely and efficiently redirected in vivo towards a specific fate, also highlighting the importance of quantitative regulation in fate choices.

### Temporal control of NSC plasticity

It is widely accepted that NSCs are multipotent precursors; however, their plastic features have not been investigated throughout their life at the cellular level. For example, the existence of a tri-potent NSC with the capacity to generate neurons, astrocytes and oligodendrocytes in the adult brain remains to be demonstrated in vivo (Williams et al., 1991). Our study demonstrates that NSCs are more plastic at early embryonic stages than at the end of embryogenesis. Furthermore, the intrinsically defined program of quiescence is not compatible with fate conversion, even though quiescent cells are subsequently reactivated. As *Drosophila* glia are generated at different stages (Halter et al., 1995) (S. Sorrentino and A.G., unpublished), it is unlikely that a general glial repressor arises late in development and specifically restricts the potential of Gcm. Our data rather imply that temporal cues progressively limit NSC plasticity, a feature that may have important consequences in therapeutic applications.

It will be of great interest to determine whether such irreversible temporal restriction relies on external cues or whether it reflects an internal clock, as it has been shown for the acquisition of temporal identity, the process by which specific progenies are produced at different developmental stages (Doe, 1992).

Finally, our data show that Gcm does not reprogram neurons. Thus, although other somatic (Vierbuchen et al., 2010) and even germ line (Tursun et al., 2011) cells can be reprogrammed into neurons, these post-mitotic cells seem endowed with an efficient brake to fate conversion. Interestingly, dorsal root ganglia neurons can transdifferentiate from one subtype into another in zebrafish, suggesting that, under some conditions, neurons can adopt a different, but closely related, phenotype (Wright et al., 2010). In addition, we cannot formally exclude that a low percentage of immature neurons adopt a glial or a multipotent phenotype upon Gcm overexpression. Nevertheless, our data indicate that neurons are intrinsically different from other cell types, which may reflect a specific chromatin organization and/or expression of an efficient tumor suppressor molecular network (for a review, see Jopling et al., 2011). Transcriptome analyses will help characterizing the molecular signature responsible for the neuronal behavior.

### Plasticity and intermediate states

Dedifferentiation and transdifferentiation of somatic cells can occur in the absence of mitosis (Richard et al., 2011), whereas NSCs plasticity has generally been associated to cell division, as a means to erase transcriptional programs and implement new ones. We here show that, like terminally differentiated cells, NSCs can be efficiently redirected in the absence of cell division. The concomitant extinction of the endogenous program and activation of the glial program indicate that conversion occurs via an intermediate state, as has been described in B cell to macrophage experimental transdifferentiation (Xie et al., 2004). The acquisition of an intermediate state (partial reprogramming) has also been proposed for somatic cell reprogramming (Hanna et al., 2009). Our findings raise a more general question as to whether intermediate states are common and unstable features of many plastic process including development. These states may reveal competing molecular pathways that in physiological conditions are alternatively consolidated or switched off in response to cell-specific signals. The development of tools enabling tracing these dynamic states will improve our understanding of cell plasticity under physiological and experimental conditions.

Interestingly, altered tumor suppressor gene expression, which alters the proliferation pathway, leads to ambiguous cell identities, which may reflect the stabilization of intermediate fates (Ma et al., 2007). Similarly, *Drosophila* metastatic cells from brain tumors (Beaucher et al., 2007) and several non-dividing NSC cells challenged with Gcm co-express the neuronal and the glial programs. We propose that the appropriate activation of the mitotic pathway is necessary for efficient consolidation/extinction of specific fates.

### Low H3K9ac and dCBP levels characterize glial cells

The interplay of extrinsic signals, transcription factors and chromatin modifications shape the identity of different cell types. The low and high levels of dCBP as well as H3K9ac truly represent a glial and neuronal signature, respectively. They both depend on *gcm*, which controls the fate choice, but not on genes downstream to Gcm, which are not sufficient to implement such choice (compare H3K9ac/dCBP levels in *gcm* embryos, with those in *repo* or *tramtrack* embryos) (Fig. 5H, Fig. 6D; data not shown). Thus, full fate conversion is accompanied by a cell-specific chromatin modification.

Interestingly, whereas dCBP accumulates at different levels in glia versus neurons and its overexpression or loss affects the levels of H3K9ac, the levels of dGCN5, another HAT that is able to

acetylate the H3K9 residue in vivo (Carre et al., 2005), are similar in glia and neurons. Moreover, dGCN5 overexpression does not enhance H3K9ac levels nor does it affect the expression of glial genes (see Fig. S8D,E in the supplementary material). These data strongly suggest that the dCBP HAT specifically participates in setting up the H3K9ac signature. It should be noted that dGCN5 is a member of multiprotein complexes (Muratoglu et al., 2003), which may explain why its overexpression cannot produce high HAT activity on its own. The balance between HATs and histone deacetylases (HDACs), enzymes with counteracting activities, is thought to be important in the regulation of histone acetylation levels. Although the investigation of histone deacetylation is not in the focus of this paper, the relevance of HDACs in the control of the glia-neuron histone acetylation signature cannot be excluded.

The tight regulation of histone acetylation in the nervous system seems to be evolutionarily conserved. Human neuronal disorders are frequently connected to downregulation of histone acetylation and HDAC inhibitors are good candidates as therapeutic tools (Lubin et al., 2011). Histone acetylation is instrumental for mammalian memory formation (Lesburgueres et al., 2011; Lubin et al., 2011) and CBP plays an important role in long-term memory processes (Barrett et al., 2011; Valor et al., 2011). Altogether, these data indicate that normal neuronal function requires high levels of histone acetylation.

Our study shows that low HAT activity is necessary for glial differentiation. The increased levels of histone acetylation by overexpression of dCBP cause downregulation of the majority (but not all) of the tested glial genes, whereas the levels of general nuclear factors remain unchanged. The glial cells do not undergo apoptosis, indicating that high dCBP and histone acetylation levels influence specific pathways rather than generally affecting cell viability. The exact molecular mechanisms are not known, yet the behavior is similar in the mammalian CNS. Oligodendrocyte differentiation requires low levels of histone acetylation, resulting from high amounts of HDACs and low amounts of HATs (CBP and P300) (Shen et al., 2005). The role of HDACs was further investigated (Shen et al., 2008; Ye et al., 2009), showing that such enzymes directly repress genes that prevent oligodendrocyte differentiation. The role of HATs was not investigated in these publications, but most probably an appropriate balance between HATs and HDACs is the key factor, which produces low levels of histone acetylation and regulates mammalian as well as *Drosophila* glial differentiation.

The broadly accepted model is that histone acetylation weakens the interaction between positively charged histone tails and negatively charged DNA, thereby contributing to transcriptional activation. Our data contradict this simple model. First, the levels of H3K4me3, a histone mark that is connected to actively transcribed genes (Lessard and Crabtree, 2010), are similar in glia and neurons. Second, the total mRNA levels are not different in the two cell populations. Third, and most importantly, dCBP overexpression in glia specifically causes downregulation of a set of glial genes. It seems that the H3K9ac levels reflect specific functional differences between neurons and glia, rather than simply revealing general gene activation. Maybe neurons require more plastic and dynamic regulation of transcription than other cell types and this process requires higher capacity of histone acetylation. Supporting this theory is the finding that a large number of activity-regulated enhancers bind CBP in cortical neuronal cultures (Kim et al., 2010). The technological breakthrough will be to analyze the transcriptome and the chromatin landscape of a few cells, which will help understanding the mode of action of dCBP and HDACs in the control of *Drosophila* glial and neuronal differentiation.

## Acknowledgements

We thank L. Tora, G. Technau, B. Altenhein, A. Mazo, S. G. Georgieva, V. Auld, J. P. Kumar, M. R. Freeman, R. Bainton, J. Skeath, M. Mannervik, V. Rodrigues, J. F. Ferveur, C. Gonzales, S. Thor, the DHSB and the Bloomington Stock Center for reagents and flies. We thank the lab members for comments on the manuscript, and C. Diebold, C. Delaporte and fly, cell separation and imaging facilities for technical assistance.

## Funding

Work was supported by INSERM, CNRS, UDS, Hôpital de Strasbourg, ARC, INCA and ANR. B.E. is supported by INSERM/Région Alsace and ARC; O.K. and P.L. are supported by FRM.

## Competing interests statement

The authors declare no competing financial interests.

## Supplementary material

Supplementary material for this article is available at <http://dev.biologists.org/lookup/suppl/doi:10.1242/dev.070391/-/DC1>

## References

- Akimaru, H., Hou, D. X. and Ishii, S. (1997). *Drosophila* CBP is required for dorsal-dependent twist gene expression. *Nat. Genet.* **17**, 211-214.
- Akiyama-Oda, Y., Hotta, Y., Tsukita, S. and Oda, H. (2000). Distinct mechanisms triggering glial differentiation in *Drosophila* thoracic and abdominal neuroblasts 6-4. *Dev. Biol.* **222**, 429-439.
- Allen, N. D. (2008). Temporal and epigenetic regulation of neurodevelopmental plasticity. *Philos. Trans. R. Soc. Lond. B* **363**, 23-38.
- Altenhein, B., Becker, A., Busold, C., Beckmann, B., Hoheisel, J. D. and Technau, G. M. (2006). Expression profiling of glial genes during *Drosophila* embryogenesis. *Dev. Biol.* **296**, 545-560.
- Bainton, R. J., Tsai, L. T., Schwabe, T., DeSalvo, M., Gaul, U. and Heberlein, U. (2005). moody encodes two GPCRs that regulate cocaine behaviors and blood-brain barrier permeability in *Drosophila*. *Cell* **123**, 145-156.
- Barrett, R. M., Malvaez, M., Kramar, E., Matheos, D. P., Arrizon, A., Cabrera, S. M., Lynch, G., Greene, R. W. and Wood, M. A. (2011). Hippocampal focal knockout of CBP affects specific histone modifications, long-term potentiation, and long-term memory. *Neuropsychopharmacology* **36**, 1545-1556.
- Baumgardt, M., Miguel-Aliaga, I., Karlsson, D., Ekman, H. and Thor, S. (2007). Specification of neuronal identities by feedforward combinatorial coding. *PLoS Biol.* **5**, e37.
- Baumgardt, M., Karlsson, D., Terriente, J., Diaz-Benjumea, F. J. and Thor, S. (2009). Neuronal subtype specification within a lineage by opposing temporal feed-forward loops. *Cell* **139**, 969-982.
- Beaucher, M., Goodliffe, J., Hersperger, E., Trunova, S., Frydman, H. and Shearn, A. (2007). *Drosophila* brain tumor metastases express both neuronal and glial cell type markers. *Dev. Biol.* **301**, 287-297.
- Beckervordersandforth, R. M., Rickert, C., Altenhein, B. and Technau, G. M. (2008). Subtypes of glial cells in the *Drosophila* embryonic ventral nerve cord as related to lineage and gene expression. *Mech. Dev.* **125**, 542-557.
- Berger, C., Renner, S., Luer, K. and Technau, G. M. (2007). The commonly used marker ELAV is transiently expressed in neuroblasts and glial cells in the *Drosophila* embryonic CNS. *Dev. Dyn.* **236**, 3562-3568.
- Berger, C., Kannan, R., Myneni, S., Renner, S., Shashidhara, L. S. and Technau, G. M. (2010). Cell cycle independent role of Cyclin E during neural cell fate specification in *Drosophila* is mediated by its regulation of Prospero function. *Dev. Biol.* **337**, 415-424.
- Bernardoni, R., Vivanco, V. and Giangrande, A. (1997). glide/gcm is expressed and required in the scavenger cell lineage. *Dev. Biol.* **191**, 118-130.
- Bernardoni, R., Miller, A. A. and Giangrande, A. (1998). Glial differentiation does not require a neural ground state. *Development* **125**, 3189-3200.
- Bier, E., Vaessin, H., Younger-Shepherd, S., Jan, L. Y. and Jan, Y. N. (1992). deadpan, an essential pan-neural gene in *Drosophila*, encodes a helix-loop-helix protein similar to the hairy gene product. *Genes Dev.* **6**, 2137-2151.
- Bossing, T., Udolph, G., Doe, C. Q. and Technau, G. M. (1996). The embryonic central nervous system lineages of *Drosophila melanogaster*. I. Neuroblast lineages derived from the ventral half of the neuroectoderm. *Dev. Biol.* **179**, 41-64.
- Campbell, G., Goring, H., Lin, T., Spana, E., Andersson, S., Doe, C. Q. and Tomlinson, A. (1994). RK2, a glial-specific homeodomain protein required for embryonic nerve cord condensation and viability in *Drosophila*. *Development* **120**, 2957-2966.
- Carre, C., Szymczak, D., Pidoux, J. and Antoniewski, C. (2005). The histone H3 acetylase dGcn5 is a key player in *Drosophila melanogaster* metamorphosis. *Mol. Cell. Biol.* **25**, 8228-8238.
- Ceron, J., Gonzalez, C. and Tejedor, F. J. (2001). Patterns of cell division and expression of asymmetric cell fate determinants in postembryonic neuroblast lineages of *Drosophila*. *Dev. Biol.* **230**, 125-138.
- Cohen, G. M. (1997). Caspases: the executioners of apoptosis. *Biochem. J.* **326**, 1-16.
- De Iaco, R., Soustelle, L., Kammerer, M., Sorrentino, S., Jacques, C. and Giangrande, A. (2006). Hucklebein-mediated autoregulation of Glide/Gcm triggers glia specification. *EMBO J.* **25**, 244-254.
- Delaunay, D., Heydon, K., Cumano, A., Schwab, M. H., Thomas, J. L., Suter, U., Nave, K. A., Zalc, B. and Spassky, N. (2008). Early neuronal and glial fate restriction of embryonic neural stem cells. *J. Neurosci.* **28**, 2551-2562.
- Dittrich, R., Bossing, T., Gould, A. P., Technau, G. M. and Urban, J. (1997). The differentiation of the serotonergic neurons in the *Drosophila* ventral nerve cord depends on the combined function of the zinc finger proteins Eagle and Hucklebein. *Development* **124**, 2515-2525.
- Doe, C. Q. (1992). Molecular markers for identified neuroblasts and ganglion mother cells in the *Drosophila* central nervous system. *Development* **116**, 855-863.
- Doe, C. Q., Fuerstenberg, S. and Peng, C. Y. (1998). Neural stem cells: from fly to vertebrates. *J. Neurobiol.* **36**, 111-127.
- Edgar, B. A. and O'Farrell, P. H. (1990). The three postblastoderm cell cycles of *Drosophila* embryogenesis are regulated in G2 by string. *Cell* **62**, 469-480.
- Egger, B., Leemans, R., Loop, T., Kammermeier, L., Fan, Y., Radimerski, T., Strahm, M. C., Certa, U. and Reichert, H. (2002). Gliogenesis in *Drosophila*: genome-wide analysis of downstream genes of glial cells missing in the embryonic nervous system. *Development* **129**, 3295-3309.
- Forsberg, M., Carlen, M., Meletis, K., Yeung, M. S., Barnabe-Heider, F., Persson, M. A., Aarum, J. and Frisen, J. (2010). Efficient reprogramming of adult neural stem cells to monocytes by ectopic expression of a single gene. *Proc. Natl. Acad. Sci. USA* **107**, 14657-14661.
- Freeman, M. R., Delrow, J., Kim, J., Johnson, E. and Doe, C. Q. (2003). Unwrapping glial biology: Gcm target genes regulating glial development, diversification, and function. *Neuron* **38**, 567-580.
- Gaspard, N. and Vanderhaeghen, P. (2011). From stem cells to neural networks: recent advances and perspectives for neurodevelopmental disorders. *Dev. Med. Child Neurol.* **53**, 13-17.
- Gibney, E. R. and Nolan, C. M. (2010). Epigenetics and gene expression. *Heredity* **105**, 4-13.
- Graf, T. and Enver, T. (2009). Forcing cells to change lineages. *Nature* **462**, 587-594.
- Grosjean, Y., Balakireva, M., Darteville, L. and Ferveur, J. F. (2001). PGa4 excision reveals the pleiotropic effects of Voila, a *Drosophila* locus that affects development and courtship behaviour. *Genet. Res.* **77**, 239-250.
- Halter, D. A., Urban, J., Rickert, C., Ner, S., Ito, K., Travers, A. A. and Technau, G. M. (1995). The homeobox gene repo is required for the differentiation and maintenance of glia function in the embryonic nervous system of *Drosophila melanogaster*. *Development* **121**, 317-332.
- Hanna, J., Markoulaki, S., Mitalipova, M., Cheng, A. W., Cassidy, J. P., Staerk, J., Carey, B. W., Lengner, C. J., Foreman, R., Love, J. et al. (2009). Metastable pluripotent states in NOD-mouse-derived ESCs. *Cell Stem Cell* **4**, 513-524.
- Higashijima, S., Shishido, E., Matsuzaki, M. and Saigo, K. (1996). eagle, a member of the steroid receptor gene superfamily, is expressed in a subset of neuroblasts and regulates the fate of their putative progeny in the *Drosophila* CNS. *Development* **122**, 527-536.
- Hosoya, T., Takizawa, K., Nitta, K. and Hotta, Y. (1995). glial cells missing: a binary switch between neuronal and glial determination in *Drosophila*. *Cell* **82**, 1025-1036.
- Hsieh, J., Nakashima, K., Kuwabara, T., Mejia, E. and Gage, F. H. (2004). Histone deacetylase inhibition-mediated neuronal differentiation of multipotent adult neural progenitor cells. *Proc. Natl. Acad. Sci. USA* **101**, 16659-16664.
- Jakob, F. (2011). New targets for treatment of osteoporosis. *Dtsch. Med. Wochenschr.* **136**, 898-903.
- Jessberger, S., Toni, N., Clemenson, G. D., Jr, Ray, J. and Gage, F. H. (2008). Directed differentiation of hippocampal stem/progenitor cells in the adult brain. *Nat. Neurosci.* **11**, 888-893.
- Jones, B. W., Fetter, R. D., Tear, G. and Goodman, C. S. (1995). glial cells missing: a genetic switch that controls glial versus neuronal fate. *Cell* **82**, 1013-1023.
- Jopling, C., Boue, S. and Izpisua Belmonte, J. C. (2011). Dedifferentiation, transdifferentiation and reprogramming: three routes to regeneration. *Nat. Rev. Mol. Cell Biol.* **12**, 79-89.
- Karlsson, D., Baumgardt, M. and Thor, S. (2010). Segment-specific neuronal subtype specification by the integration of anteroposterior and temporal cues. *PLoS Biol.* **8**, e1000368.
- Kim, J. B., Sebastiano, V., Wu, G., Arauzo-Bravo, M. J., Sasse, P., Gentile, L., Ko, K., Ruau, D., Ehrlich, M., van den Boom, D. et al. (2009). Oct4-induced pluripotency in adult neural stem cells. *Cell* **136**, 411-419.
- Kim, T. K., Hemberg, M., Gray, J. M., Costa, A. M., Bear, D. M., Wu, J., Harmin, D. A., Laptewicz, M., Barbara-Haley, K., Kuersten, S. et al. (2010). Widespread transcription at neuronal activity-regulated enhancers. *Nature* **465**, 182-187.

- Kokubo, T., Gong, D. W., Wootton, J. C., Horikoshi, M., Roeder, R. G. and Nakatani, Y. (1994). Molecular cloning of *Drosophila* TFIIID subunits. *Nature* **367**, 484-487.
- Kumar, J. P., Jamal, T., Doetsch, A., Turner, F. R. and Duffy, J. B. (2004). CREB binding protein functions during successive stages of eye development in *Drosophila*. *Genetics* **168**, 877-893.
- Landgraf, M., Sanchez-Soriano, N., Technau, G. M., Urban, J. and Prokop, A. (2003). Charting the *Drosophila* neuropile: a strategy for the standardised characterisation of genetically amenable neurites. *Dev. Biol.* **260**, 207-225.
- Lebedeva, L. A., Nabirochkina, E. N., Kurshakova, M. M., Robert, F., Krasnov, A. N., Evgen'ev, M. B., Kadonaga, J. T., Georgieva, S. G. and Tora, L. (2005). Occupancy of the *Drosophila* hsp70 promoter by a subset of basal transcription factors diminishes upon transcriptional activation. *Proc. Natl. Acad. Sci. USA* **102**, 18087-18092.
- Lee, B. P. and Jones, B. W. (2005). Transcriptional regulation of the *Drosophila* glial gene repo. *Mech. Dev.* **122**, 849-862.
- Lesburgueres, E., Gobbo, O. L., Alaux-Cantin, S., Hambucken, A., Trifileff, P. and Bontempi, B. (2011). Early tagging of cortical networks is required for the formation of enduring associative memory. *Science* **331**, 924-928.
- Lessard, J. A. and Crabtree, G. R. (2010). Chromatin regulatory mechanisms in pluripotency. *Annu. Rev. Cell Dev. Biol.* **26**, 503-532.
- Lilja, T., Qi, D., Stabell, M. and Mannervik, M. (2003). The CBP coactivator functions both upstream and downstream of Dpp/Screw signaling in the early *Drosophila* embryo. *Dev. Biol.* **262**, 294-302.
- Lubin, F. D., Gupta, S., Parrish, R. R., Grissom, N. M. and Davis, R. L. (2011). Epigenetic mechanisms: critical contributors to long-term memory formation. *Neuroscientist* (in press).
- Ma, L., Hocking, J. C., Hehr, C. L., Schuurmans, C. and McFarlane, S. (2007). Zac1 promotes a Muller glial cell fate and interferes with retinal ganglion cell differentiation in *Xenopus* retina. *Dev. Dyn.* **236**, 192-202.
- McGuire, S. E., Le, P. T., Osborn, A. J., Matsumoto, K. and Davis, R. L. (2003). Spatiotemporal rescue of memory dysfunction in *Drosophila*. *Science* **302**, 1765-1768.
- Miller, A. A., Bernardoni, R. and Giangrande, A. (1998). Positive autoregulation of the glial promoting factor glide/gcm. *EMBO J.* **17**, 6316-6326.
- Mollinari, C., Lange, B. and Gonzalez, C. (2002). Miranda, a protein involved in neuroblast asymmetric division, is associated with embryonic centrosomes of *Drosophila melanogaster*. *Biol. Cell* **94**, 1-13.
- Morshead, C. M., Reynolds, B. A., Craig, C. G., McBurney, M. W., Staines, W. A., Morassutti, D., Weiss, S. and van der Kooy, D. (1994). Neural stem cells in the adult mammalian forebrain: a relatively quiescent subpopulation of subependymal cells. *Neuron* **13**, 1071-1082.
- Muratoglu, S., Georgieva, S., Papai, G., Scheer, E., Enunlu, I., Komonyi, O., Cserpan, I., Lebedeva, L., Nabirochkina, E., Udvardy, A. et al. (2003). Two different *Drosophila* ADA2 homologues are present in distinct GCN5 histone acetyltransferase-containing complexes. *Mol. Cell. Biol.* **23**, 306-321.
- Puvion-Dutilleul, F., Besse, S., Diaz, J. J., Kindbeiter, K., Vigneron, M., Warren, S. L., Keding, C., Madjar, J. J. and Puvion, E. (1997). Identification of transcription factories in nuclei of HeLa cells transiently expressing the Us11 gene of herpes simplex virus type 1. *Gene Expr.* **6**, 315-332.
- Qi, D., Larsson, J. and Mannervik, M. (2004). *Drosophila* Ada2b is required for viability and normal histone H3 acetylation. *Mol. Cell. Biol.* **24**, 8080-8089.
- Richard, J. P., Zury, S., Fischer, N., Pavet, V., Vaucamps, N. and Jarriault, S. (2011). Direct in vivo cellular reprogramming involves transition through discrete, non-pluripotent steps. *Development* **138**, 1483-1492.
- Rivers, L. E., Young, K. M., Rizzi, M., Jamen, F., Psachoulia, K., Wade, A., Kessaris, N. and Richardson, W. D. (2008). PDGFRA/NG2 glia generate myelinating oligodendrocytes and piriform projection neurons in adult mice. *Nat. Neurosci.* **11**, 1392-1401.
- Rowitch, D. H. and Kriegstein, A. R. (2010). Developmental genetics of vertebrate glial-cell specification. *Nature* **468**, 214-222.
- Schmidt, H., Rickert, C., Bossing, T., Vef, O., Urban, J. and Technau, G. M. (1997). The embryonic central nervous system lineages of *Drosophila melanogaster*. II. Neuroblast lineages derived from the dorsal part of the neuroectoderm. *Dev. Biol.* **189**, 186-204.
- Sen, A., Shetty, C., Jhaveri, D. and Rodrigues, V. (2005). Distinct types of glial cells populate the *Drosophila* antenna. *BMC Dev. Biol.* **5**, 25.
- Sepp, K. J., Schulte, J. and Auld, V. J. (2001). Peripheral glia direct axon guidance across the CNS/PNS transition zone. *Dev. Biol.* **238**, 47-63.
- Shen, C. P., Jan, L. Y. and Jan, Y. N. (1997). Miranda is required for the asymmetric localization of Prospero during mitosis in *Drosophila*. *Cell* **90**, 449-458.
- Shen, S., Li, J. and Casaccia-Bonnel, P. (2005). Histone modifications affect timing of oligodendrocyte progenitor differentiation in the developing rat brain. *J. Cell Biol.* **169**, 577-589.
- Shen, S., Sandoval, J., Swiss, V. A., Li, J., Dupree, J., Franklin, R. J. and Casaccia-Bonnel, P. (2008). Age-dependent epigenetic control of differentiation inhibitors is critical for remyelination efficiency. *Nat. Neurosci.* **11**, 1024-1034.
- Sousa-Nunes, R., Yee, L. L. and Gould, A. P. (2011). Fat cells reactivate quiescent neuroblasts via TOR and glial insulin relays in *Drosophila*. *Nature* **471**, 508-512.
- Soustelle, L. and Giangrande, A. (2007). Glial differentiation and the Gcm pathway. *Neuron Glia Biol.* **3**, 5-16.
- Tsui, T., Hasegawa, E. and Isshiki, T. (2008). Neuroblast entry into quiescence is regulated intrinsically by the combined action of spatial Hox proteins and temporal identity factors. *Development* **135**, 3859-3869.
- Tursun, B., Patel, T., Kratsios, P. and Hobert, O. (2011). Direct conversion of *C. elegans* germ cells into specific neuron types. *Science* **331**, 304-308.
- Valor, L. M., Pulopulos, M. M., Jimenez-Minchan, M., Olivares, R., Lutz, B. and Barco, A. (2011). Ablation of CBP in forebrain principal neurons causes modest memory and transcriptional defects and a dramatic reduction of histone acetylation but does not affect cell viability. *J. Neurosci.* **31**, 1652-1663.
- Vierbuchen, T., Ostermeier, A., Pang, Z. P., Kokubu, Y., Sudhof, T. C. and Wernig, M. (2010). Direct conversion of fibroblasts to functional neurons by defined factors. *Nature* **463**, 1035-1041.
- Vincent, S., Vonesch, J. L. and Giangrande, A. (1996). Glide directs glial fate commitment and cell fate switch between neurones and glia. *Development* **122**, 131-139.
- von Hilchen, C. M., Hein, I., Technau, G. M. and Altenhein, B. (2010). Netrins guide migration of distinct glial cells in the *Drosophila* embryo. *Development* **137**, 1251-1262.
- Wang, J., Weaver, I. C., Gauthier-Fisher, A., Wang, H., He, L., Yeomans, J., Wondisford, F., Kaplan, D. R. and Miller, F. D. (2010). CBP histone acetyltransferase activity regulates embryonic neural differentiation in the normal and Rubinstein-Taybi syndrome brain. *Dev. Cell* **18**, 114-125.
- Williams, B. P., Read, J. and Price, J. (1991). The generation of neurons and oligodendrocytes from a common precursor cell. *Neuron* **7**, 685-693.
- Wright, M. A., Mo, W., Nicolson, T. and Ribera, A. B. (2010). In vivo evidence for transdifferentiation of peripheral neurons. *Development* **137**, 3047-3056.
- Xie, H., Ye, M., Feng, R. and Graf, T. (2004). Stepwise reprogramming of B cells into macrophages. *Cell* **117**, 663-676.
- Xu, W., Edmondson, D. G. and Roth, S. Y. (1998). Mammalian GCN5 and P/CAF acetyltransferases have homologous amino-terminal domains important for recognition of nucleosomal substrates. *Mol. Cell. Biol.* **18**, 5659-5669.
- Ye, F., Chen, Y., Hoang, T., Montgomery, R. L., Zhao, X. H., Bu, H., Hu, T., Taketo, M. M., van Es, J. H., Clevers, H. et al. (2009). HDAC1 and HDAC2 regulate oligodendrocyte differentiation by disrupting the beta-catenin-TCF interaction. *Nat. Neurosci.* **12**, 829-838.